University of Baghdad
College of Engineering
JE
JOURNAL OF ENGINEERING

Journal of Engineering

journal homepage: www.jcoeng.edu.iq

Volume 31 Number 1 January 2025

Modeling Asphaltene Precipitation-Part II: Comparative Study for Asphaltene Precipitation Curve Prediction Methods

Ali A. Ali [1, 2, *], **Ghassan H. Abdul-Majeed** [3]

[1]Department of Petroleum Engineering, College of Engineering, University of Baghdad, Baghdad, Iraq
[2]Department of Oil and Gas Engineering, University of Technology, Baghdad, Iraq
[3]College of Engineering, University of Baghdad, Baghdad, Iraq

ABSTRACT

Asphaltenes' solubility in crude oils is frequently affected by temperature, pressure, and oil composition changes. This could lead to the precipitation and deposition of asphaltene in various parts of the total production system, which would cause a significant economic impact. Predicting the conditions of asphaltene precipitation will be very useful in two cases. In the first case, without the problem, it will be useful in specifying the optimum operating conditions of oil production operations. In the second case, with the problem occurring, the prediction model will be useful in knowing the deposition areas and their sizes. This study is an extension of the first part, in which the advanced versions of Peng-Robinson (APR78 EOS) and Soave-Redlich-Kwong (ASRK EOS) cubic equations of state and cubic-plus-association equations of state (CPA EOS) were compared in predicting asphaltene precipitation conditions by using Multiflash software. The prediction was made for live crude oil (API gravity = 24° API) from an Iraqi oil field at different temperatures. The required data for modeling are fluid compositional analysis, PVT experiment data, and flow assurance data, which were collected from a fluid analysis report. It was noticed that the agreement in prediction was very high between the ASRK EOS and the CPA EOS for all temperature values and diverged from the APR78 EOS model at low temperatures (T = 50 and 40 °C). This study demonstrates the impact of selecting the appropriate model on predicting asphaltene precipitation and its influence on future predictions of the asphaltene deposition problem.

Keywords: Asphaltene onset pressure, Asphaltene precipitation, Concentration, Flow assurance, Cubic equation of state.

1. INTRODUCTION

The precipitation of heavy organics during the production, transportation, and refining or processing of crude oil is one of the key issues facing the oil industry. Polar and organic

*Corresponding author
Peer review under the responsibility of University of Baghdad.
https://doi.org/10.31026/j.eng.2025.01.03

Article received: 19/05/2024
Article revised: 10/07/2024
Article accepted: 22/07/2024
Article published: 01/01/2025

molecules known as asphaltenes are stabilized in crude oil by resins. Asphaltenes are, by definition, only a solubility class, namely the heptane insoluble portion of the vacuum residue recovered from the crude oil after refining. The melting temperature of asphaltenes, which are friable solids that range from dark brown to black, is unknown. The concentration of resins decreases as the oil is diluted by light hydrocarbons, and at some point, the asphaltene may no longer be stabilized and flocculate to create a solid deposit **(Pfeiffer and Saal, 1940; Alian et al., 2011; Vakili-Nezhaad, 2013)**. Modeling studies for asphaltene by using equation of state (EOS) models began in the 1980s. Previous studies dealt with determining the phase diagram of asphaltene with the fluid to determine precipitation conditions **(Alves et al., 1991; Zhang et al., 2012; Arya et al., 2016; Ali et al., 2019a; Shoukry et al., 2020; Ahmed et al., 2023b)**, as well as studying the relationship of the precipitation curve with pressure **(Victorov and Firoozabadi, 1996; Vafaie-Sefti et al., 2003; Shirani et al., 2012; Zhang et al., 2012; Izadpanahi et al., 2019; Hajizadeh et al., 2020; Shoukry et al., 2020)**.

The problems of asphaltenes and their instability and precipitation appeared in some oil fields in Iraq. Some of the studies were focused on determining the precipitation envelope and precipitation curve of Iraqi oils from different oil reservoirs and fields, depending on real field data **(Ali et al., 2019a; Abdulwahab et al., 2020; Ali, 2021; Ahmed et al., 2023b, 2023a)**. The asphaltene stability in Iraqi crude oils (dead and live oils) was predicted by using different screening techniques to show its tendency to precipitate asphaltene **(Ali et al., 2019b; Hasan and Al-haleem, 2020; Alhuraishawy et al., 2023)**. It has been studied how the ratio of oil resins to asphaltene (R/A) affects the stability of Iraqi water in crude oil emulsions. The findings demonstrated that the emulsion will become unstable and remove more water from the emulsion as the R/A ratio rises **(Mohammed and Maan, 2016)**. **Farhan et al. (2020)** used three local solvents, which are heavy naphtha, reformate, and binary (a mixture of both reformate and heavy naphtha), to reduce the permeability damage of three sand pack samples after asphaltene precipitation. They found that the binary solution is the best solvent for asphaltene dissolving and permeability improvement. (**Ali and Naife, 2021)** treated dead oil samples from the Al-Dura refinery to remove asphaltene by using three different solvents n-hexane, n-heptane, and light naphtha via deasphalting process. The impact of several operating parameters, including temperature, solvent concentration, ratio of solvent to oil, and duration, was examined. They discovered that using hexane solvent resulted in a larger reduction in asphaltene content. (**Kasim and Abbas, 2022)** performed SARA analysis of a crude oil sample from the field of the Omar River with different additives of nanoparticles and polymer fiberglass to decrease asphaltene content. The effect of additive concentrations and temperature was examined. They noticed that the nanoparticles were better than polymer fiberglass in reducing the asphaltene content of the crude oil. (**Maddah and Naife, 2019)** mentioned the effect of asphaltene content on the process of water demulsification during their study using two different types of crude oil, one from Basrah and the other from Kirkuk.

Previous research indicates that the precipitated asphaltenes behave more like liquids than solids at the reservoir temperature. At ambient temperature, the solid phase assumption is most likely correct, but at high temperatures, it might not be. Based on this supposition, several researchers treat the precipitation of asphaltene as a liquid-liquid (LLE) equilibrium mechanism **(Wu et al., 1998, 2000; Firoozabadi, 1999; Buenrostro-Gonzalez et al., 2004; Gonzalez et al., 2005; Duda and Lira-Galeana, 2006; Tharanivasan et al., 2009; Li and Firoozabadi, 2010)**.

In this study, the liquid-liquid (LLE) computation was used. The contribution of the present research is to show the differences between the mentioned cubic equation of state models (CPA EOS, ASRK EOS, and APR78 EOS) in predicting the asphaltene concentration of a live oil as a function of pressure and temperature. The main conclusion of this paper is that there was a clear discrepancy or difference between the APR78 EOS model and the models of ASRK EOS and CPA EOS in predicting the curves of asphaltene precipitation at lower temperatures, and this difference will affect the asphaltene deposition modeling at the low-temperature points in the production tubings and pipelines.

2. THE USED MODELS OF EQUATION OF STATES

In this study, two types of equations of state were used to predict the asphaltene precipitation curve (asphaltene concentration versus pressure relationship) by matching the experimental data of both the fluid and solid (asphaltene) phases.
1- Cubic Equation of State: The general form of the cubic equation of state is illustrated in Eq. (1) **(Pedersen et al., 2006)**.

$$p = \frac{RT}{v-b} - \frac{a}{v^2+vb(1+c)-cb^2} \quad (1)$$

- Advanced Peng-Robinson78 Equation of State (APR78 EOS): When c=1, Eq. (1) becomes the Peng-Robinson equation of state **(Robinson and Peng, 1978)**.
- Advanced Soave-Redlich-Kwong Equation of State (ASRK EOS): When c=0, Eq. (1) becomes the Soave-Redlich-Kwong equation of state **(Soave, 1972)**.

It is possible to match saved values for saturated vapor pressure and liquid density in the advanced version, which also offers an option for mixing rules.

2- Cubic-Plus-Association Equation of State (CPA EOS): Equation (1) becomes Cubic-Plus-Association Equation of State (CPA EOS) by adding the association portion and changing c to zero as shown in Eq. (2) **(Kontogeorgis et al., 1996; Kontogeorgis et al., 1999)**.

$$p = \frac{RT}{v-b} - \frac{a}{v(v+b)} - \frac{1}{2}\frac{RT}{v}\left(1+\rho\frac{\partial \ln g}{\partial \rho}\right)\sum_i x_i \sum_{Ai}(1-x_{Ai}) \quad (2)$$

The two components of Eq. (2) are the physical part, which is the representation of the SRK EOS equation and is computed similarly to the SRK equation with the same parameters for pure compounds and mixing procedures, and the association part, which is the second part. For more details about these three models, you can review the first part of the study **(Ali and Abdul-Majeed, 2024)**.

3. THE METHODOLOGY

The required data for asphaltene precipitation modeling of the live oil are:
1- Compositional analysis of the live oil.
2- PVT experimental data of the live oil.
3- SARA analysis data for the fluid.
4- Upper and lower asphaltene onset pressures.

The above data were collected from the fluid analysis report of a well produced from the Mishrif Formation in the Buzurgan oil field and are shown in **Tables 1** and **2 (Comer and Weller, 2019)**.

Table 1. The live oil composition.

Comp.	mole%	Comp.	mole%	Comp.	mole%	Comp.	mole%
N_2	0.467	Benzene	0.128	C_{14}	1.338	C_{26}	0.387
H_2S	0.981	C_7	2.882	C_{15}	1.192	C_{27}	0.36
CO_2	2.678	Toluene	0.35	C_{16}	1.055	C_{28}	0.343
C_1	35.708	C_8	2.627	C_{17}	1.017	C_{29}	0.323
C_2	9.471	Ethylbenzene	0.115	C_{18}	0.898	C_{30}	0.297
C_3	6.089	m- and p-Xylenes	0.302	C_{19}	0.654	C_{31}	0.284
i-C_4	1.035	o- Xylene	0.204	C_{20}	0.732	C_{32}	0.251
n-C_4	3.504	C_9	2.08	C_{21}	0.651	C_{33}	0.235
neo-Pentane	0.013	C_{10}	2.309	C_{22}	0.572	C_{34}	0.218
i-C_5	1.488	C_{11}	1.981	C_{23}	0.513	C_{35}	0.205
n-C_5	2.048	C_{12}	1.66	C_{24}	0.455	C_{36^+}	4.922
C_6	3.07	C_{13}	1.494	C_{25}	0.414		

Table 2. Main properties of the fluid and reservoir and operating conditions.

Item	Value	Unit
Initial reservoir pressure	5000	psi
Current reservoir pressure	4410	psi
Reservoir temperature	111	°C
Wellhead pressure	203	psi
Wellhead temperature	23.9	°C
Gas-Oil Ratio	743	SCF/bbl of residual oil at 60°F
Stocktank Oil Density	0.9059	g cm^{-3} at 0 psig and 60 °F
Bubble Point Pressure at 111 °C	3135	psi
Saturates	31.7	wt%
Aromatics	43.5	wt%
Resin	19.8	wt%
Asphaltenes	8.82	wt%
Upper AOP at 80 °C	3800	psi
Upper AOP at 110 °C	4000	psi
Upper AOP at 116 °C	3800	psi

The work methodology is a continuation of what was explained in the first part, where only the prediction of asphaltene concentration (asphaltene concentration curve) versus pressure at different temperatures using the three models is added here. The overall procedures for modeling the asphaltene precipitation curve by using Multifash software are shown in a block diagram in **Fig. 1**. These steps for each model can be summarized as follows:

1-Selecting the model and specifying the appropriate units: This step specified the model for predicting the asphaltene precipitation curve and appropriate units for input data as in the fluid analysis report.

2- Identifying the fluid composition and SARA fractions weight percentages: In this step, the fluid analysis data of the live oil, as shown in **Table 1**, and the SARA analysis data, as shown in **Table 2**, were entered into the software.

3-Fluid characterizing (applying splitting and lumping processes): In this step, the two important processes (splitting and lumping) were applied using the selected model. Splitting means defining the mole fractions of the pseudo component (C36+ in this study) depending on the correlations for each model while lumping refers to setting the split components in groups to speed up the simulation process.

4- Tuning the model for the experimental data of PVT tests: After step 3, the model predicts the phase diagrams of the fluid and asphaltene, as well as the PVT experimental data, but they are inaccurate and need a calibration process with the laboratory data of the PVT experiments, which is called the tuning or regression process. In this step, all experimental data for PVT was entered and matched.

5- Fine-tuning the model for asphaltene onset pressures: The model requires an additional tuning process for the asphaltene phase by entering the experimental data of asphaltene onset pressures and matching them with the simulated or predicted data.

6- Predicting asphaltene precipitation curve: After obtaining a reasonable and acceptable match with the laboratory results for the asphaltene onset pressure curve (AOP curve) and bubble point pressure curve, the model can predict the deposition curve, which represents the ratio of precipitated asphaltene versus pressure at any temperature.

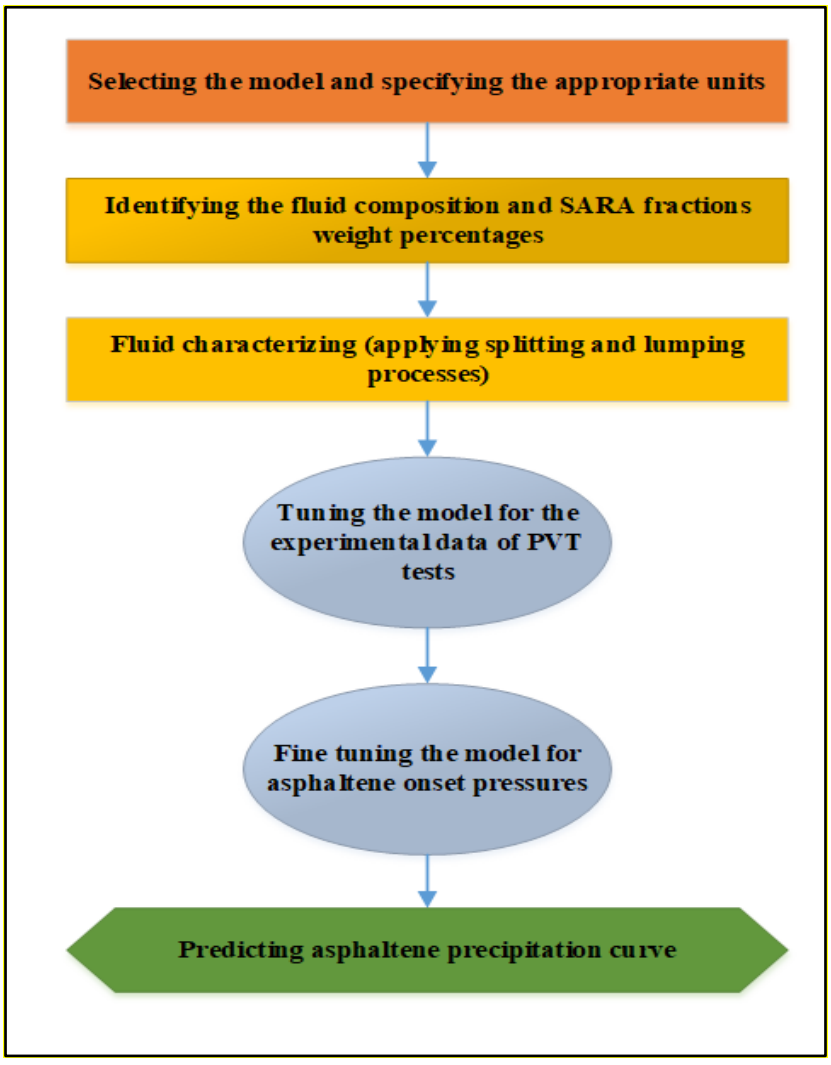

Figure 1. The overall procedures of the simulation process.

The algorithm for predicting the asphaltene precipitation curve in the Multiflash software is shown in the flow chart in **Fig. 2 (Shirani et al., 2012)**. The steps of this algorithm can be illustrated as follows:

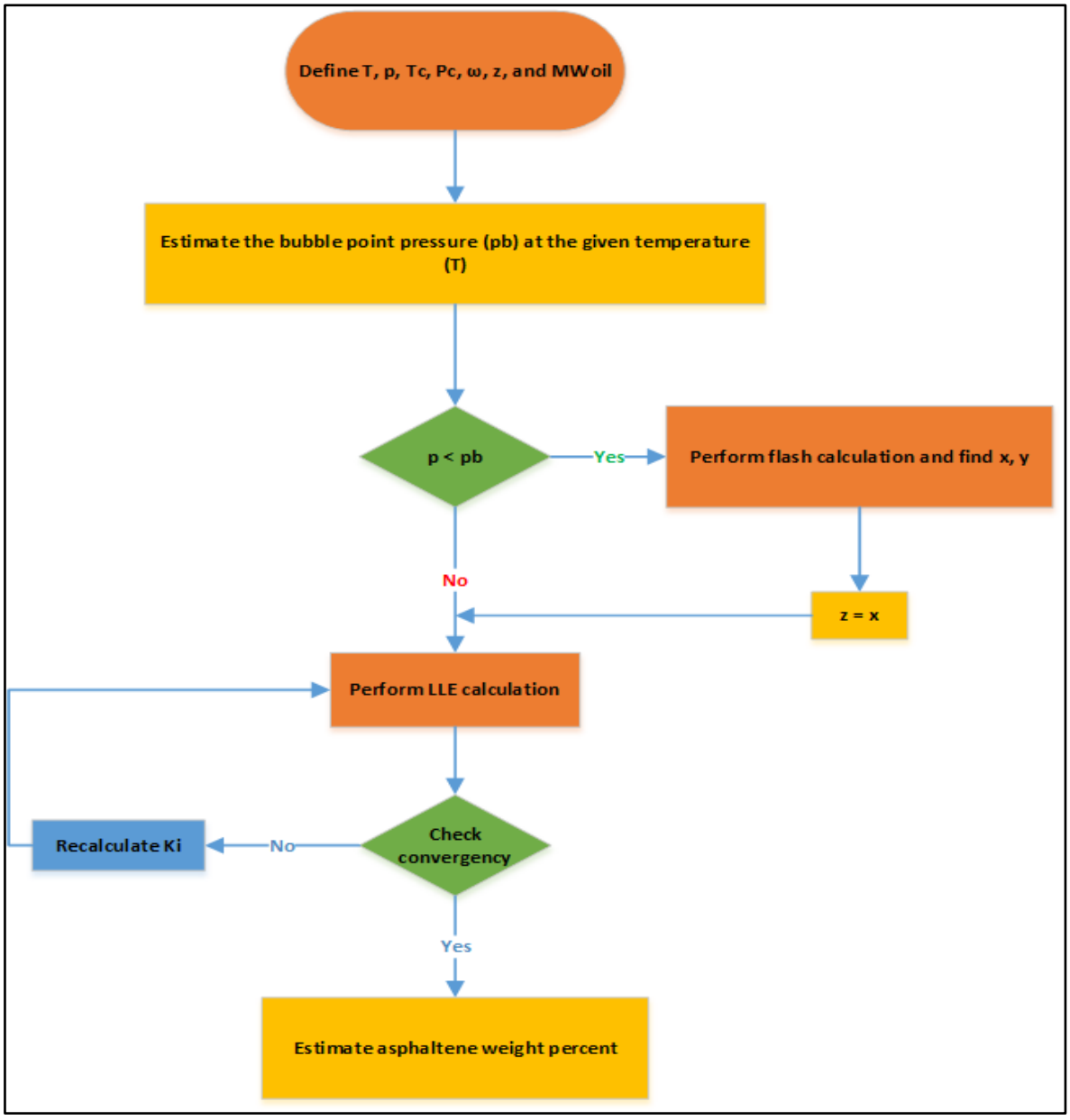

Figure 2. The flowchart of asphaltene precipitation calculation.

1- After defining the main properties, such as critical pressure and temperature (p_c, T_c), acentric factor (ω), the overall mole fraction of the fluid (z), the molecular weight of the fluid, and the conditions such as pressure and temperature, the bubble point pressure must be estimated at the given temperature.
2- The bubble point pressure estimated in the previous step is compared to the given pressure. If the estimated bubble point pressure exceeds the given pressure, the flash calculation of two phases (liquid and gas) will occur, where the overall mole fraction of the fluid (z) will be equal to the liquid mole fraction (x). Subsequently, the liquid-liquid

(LLE) calculation will be performed. If the estimated bubble point pressure is less than the given pressure, the liquid-liquid (LLE) calculation will be applied directly.

3- Performing liquid-liquid (LLE) calculation, during which the following were estimated:
1. Ki.
2. L_2/F.
3. $x_i^{L_1}$ and $x_i^{L_2}$.
4. $f_i^{L_1}$ and $f_i^{L_2}$ (i = Asphaltene, Resin).

4- The convergence was checked by the following procedure:

If $\sum_i^2 (1 - \frac{f_i^{L_2}}{f_i^{L_1}})^2 > 10^{-4}$ then

Estimate new Ki from:

$$K_i = \frac{\emptyset_i^{L_1}}{\emptyset_i^{L_2}} \quad (3)$$

and return to step 3.

Otherwise, the precipitated asphaltene percent will be obtained from:

$$\boldsymbol{x_{wi} = x_i^{L_2} \times \frac{L_2}{F} \times \frac{MW_i}{MW_{oil}}} \quad (4)$$

4. RESULTS AND DISCUSSION

In this study, the three most famous models in asphaltene precipitation modeling were addressed to compare them and determine the extent of convergence and divergence between them. This will be useful for knowing and choosing the most appropriate model for future studies, as asphaltene precipitation modeling is very important in studying the locations of asphaltene deposition and its thickness. Thus, it becomes clear to the reader where the difference will be and the importance of choosing the most appropriate model to study this very sensitive and complex problem.

After matching the experimental data of upper asphaltene onset pressure and bubble point pressure of the fluid by these models of EOS, as illustrated in **Fig. 3**, the simulation of the asphaltene precipitation curve was made. From **Fig. 3**, it is noticed that there is a good agreement between the simulated and experimental data of upper AOP and bubble point pressure after fluid characterization and tuning processes of the fluid and asphaltene by using the EOS models. The acceptable tuning process of these two important properties of the fluid and asphaltene will become an indication for the successful simulation process of predicting asphaltene precipitation curves at different temperatures.

The three models gave the following results of asphaltene precipitation curves for different temperature values, as shown in the figures below. It was observed from **Figs. 4 and 5** that there is a very large match between the three models in predicting the asphaltene precipitation curve at temperatures of 111 ˚C and 70 ˚C, respectively, with a very slight discrepancy that is almost invisible at temperatures of 70 ˚C. When the temperature is at reservoir temperature, which equals 111 ˚C, the maximum asphaltene mass% is at the bubble point pressure (3128 psia) that equals 0.29 while for the temperature of 70 ˚C, the maximum asphaltene mass% is at the bubble point pressure (2780 psia) that equals 0.24.

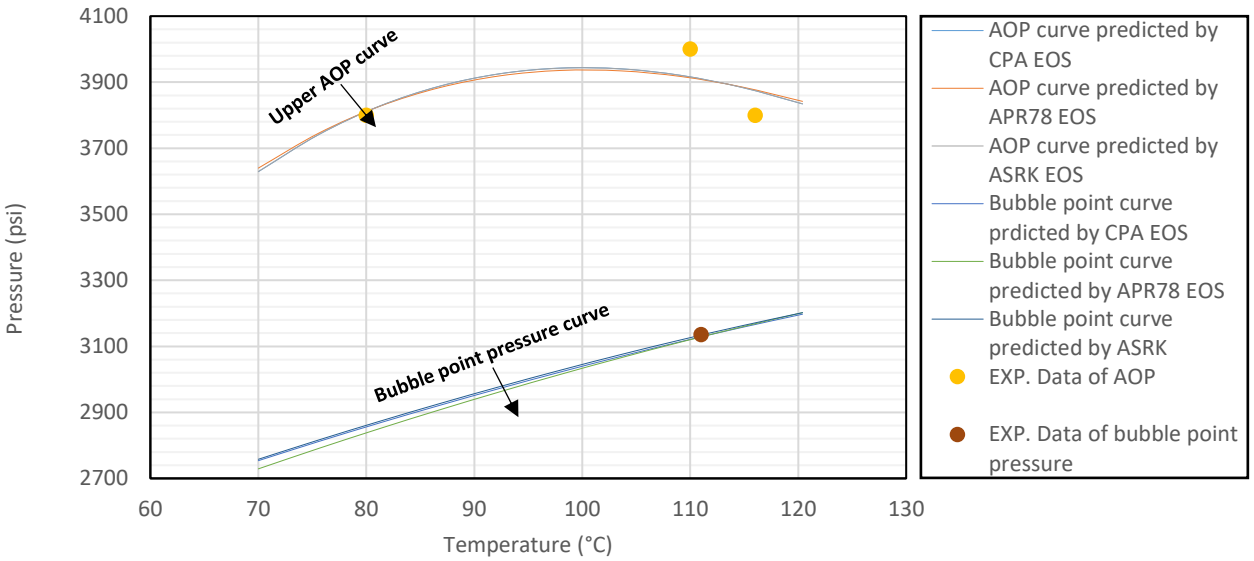

Figure 3. The predicted and experimental curves of upper AOP and bubble point pressure.

The experimental value of the bubble point pressure of the oil was 3135 psia at a temperature of 111 ˚C and by simulation process was 3128 psia at the same temperature this result is more acceptable for predicting the asphaltene precipitation curves by using EOS models.

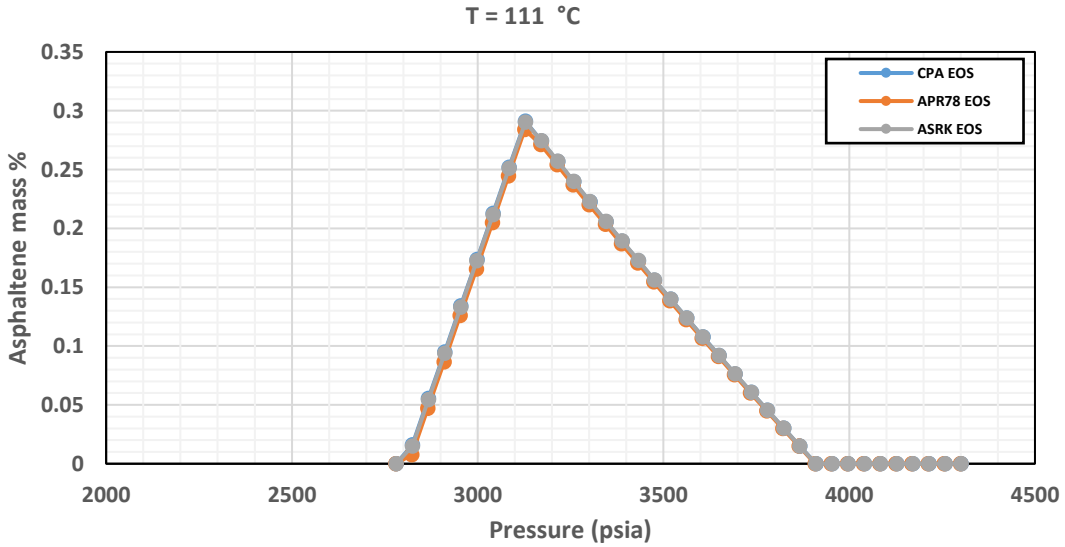

Figure 4. Asphaltene precipitation curve at 111 ˚C.

In **Figs. 6 and 7**, it was shown that the ASRK EOS and CPA EOS models were also completely identical and largely diverged from the APR78 EOS model when predicting the asphaltene precipitation curve at 50 ˚C and 40 ˚C, respectively, especially when the pressure exceeded the bubble point pressure at these two temperatures. At a temperature of 50 ˚C, the ASRK EOS and CPA EOS models gave a maximum asphaltene mass% of 0.12 at a bubble point pressure of 2530 psia while the maximum asphaltene mass% of the APR78 EOS model is 0.135 at a bubble point pressure of 2500 psia as shown in **Fig. 4**.

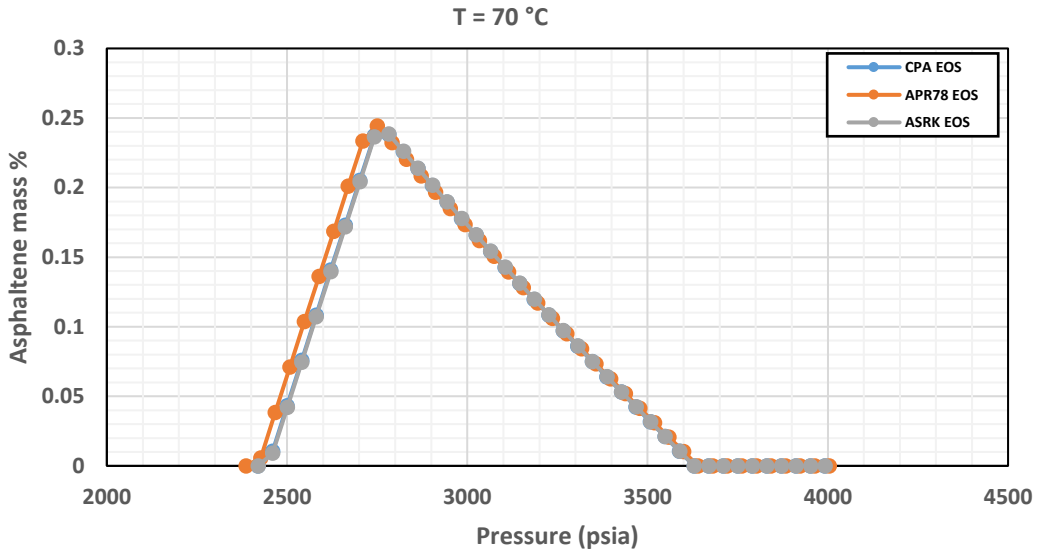

Figure 5. Asphaltene precipitation curve at 70 ˚C.

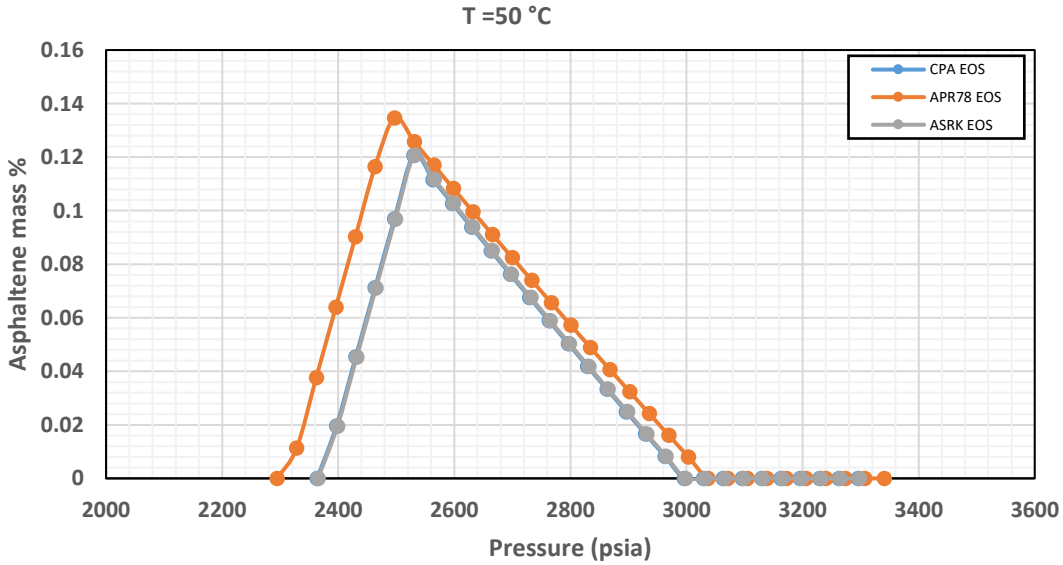

Figure 6. Asphaltene precipitation curve at 50 ˚C.

When the temperature was decreased to 40 ˚C, the large discrepancy between the model results as well as the decrease in the concentration of precipitated asphaltene appeared, as shown in **Fig.7**. The maximum asphaltene mass% by both two models (ASRK EOS and CPA EOS) is 0.028 at the bubble point pressure of 2420 psia, and it equals 0.06 at the bubble point pressure of 2360 psia. From previous figures, it was noticed there is a diverge in predicting the precipitation curves at the low temperatures between APR78 EOS and both models of ASRK EOS and CPA EOS. The reason for this behavior can be attributed to the limitations of these models. The selection of the precipitation model will affect asphaltene deposition prediction therefore it must consider these limitations before choosing the model, especially at lower temperatures. Because the ASRK EOS and CPA EOS models gave completely identical results for all temperatures, the CPA model was chosen to predict the asphaltene precipitation curve for more temperature values, starting from the reservoir temperature up to the surface temperature, as shown in **Fig. 8**.

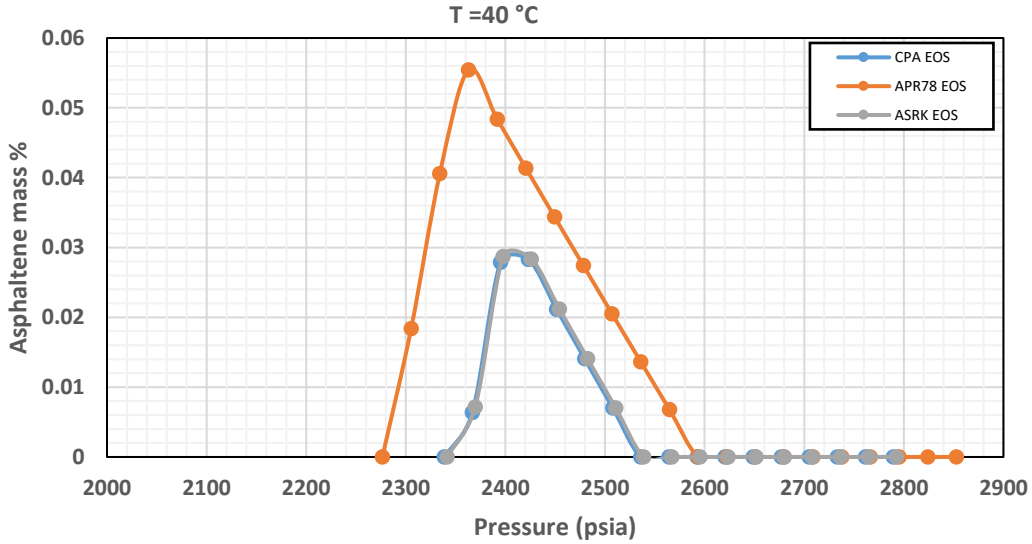

Figure 7. Asphaltene precipitation curve at 40 ˚C.

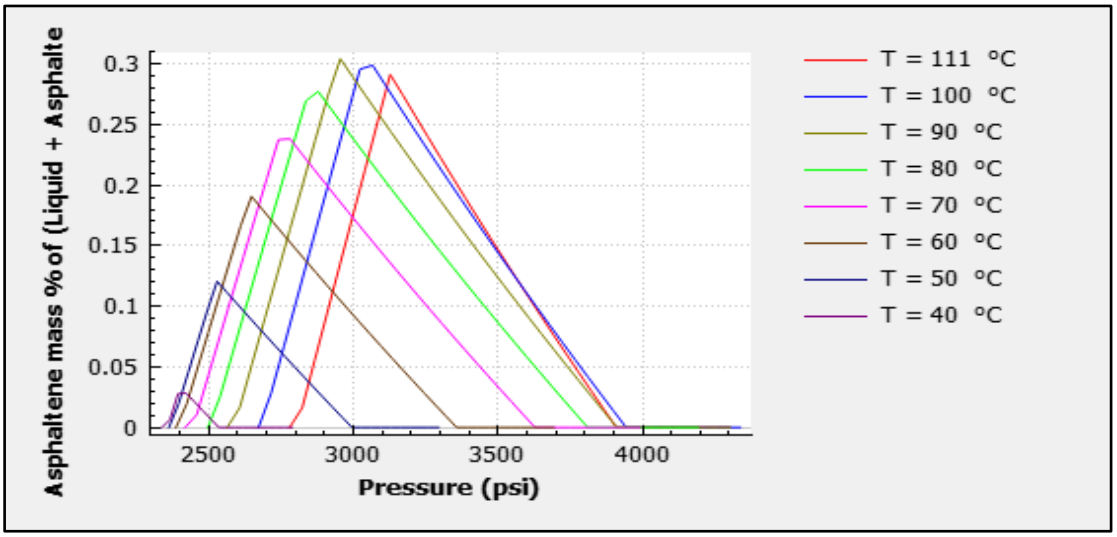

Figure 8. Asphaltene precipitation curves prediction by CPA EOS model.

It can be observed from this figure that there is an increase in asphaltene precipitation at all bubble point pressures and for all temperatures. There is also an increase in the precipitation as the pressure decreases and approaches the bubble point pressure and decreases after crossing this pressure. This is due to the dissolution property of asphaltene in oil before and after the bubble point pressure according to studies by **(Tavakoldavani and Ashoori, 2017; Jamaluddin et al., 2002)**. The asphaltene precipitates from oil before bubble point pressure because of gas liberation with decreasing pressure which causes density reduction of oil and returns to dissolve in oil after bubble point pressure due to increasing oil density after gas separation from oil. If the figure is carefully looked at, it can be seen that there is an increase in the concentration of asphaltene precipitation with a decrease in temperature, reaching a temperature of 90 ˚C, and then the deposition area gets smaller little by little, reaching the lowest concentration curve at a temperature of 40 ˚C. These results are consistent with the results of previous studies **(Hirschberg et al., 1984;**

Afshari et al., 2010; Hasanvand and Kharat, 2014). The maximum concentration of asphaltene is at higher temperatures (111, 100, and 90 ˚C) which equals approximately 0.3, and then decreases step by step until reaching 0.025 at a temperature of 40 ˚C. Therefore, it is expected that there will be asphaltene deposition in areas where the temperature is within these limits.

5. CONCLUSIONS

After achieving the study objective, which is to compare the three mentioned models of cubic state equations in studying this complex and common problem during oil production operations, which is the problem of asphaltene precipitation, the following points can be concluded:

1. There was a discrepancy or difference between the APR78 EOS and the models ASRK EOS and CPA EOS in predicting the curves of asphaltene precipitation at lower temperatures.
2. The two models ASRK EOS and CPA EOS gave the same results in simulating and determining the precipitation curves for all temperature values. This means that there is not a very clear effect of the association part that was added to the CPA EOS model, and it did not achieve a significant difference from the model without this part (ASRK EOS).
3. Given the critical role that asphaltene deposition plays in the oil production system, accurately modeling and simulating this process is essential for identifying potential deposition locations and thickness. This information can then be used to optimize production processes and mitigate flow assurance issues, thus enhancing overall efficiency and productivity.
4. The increase in the weight percentage of precipitated asphaltene before the bubble point pressure is due to the dilution of the oil with the formation of gas inside the oil, and the highest percentage of precipitation occurs at the bubble point pressure because the oil is the lightest possible in this region, and thus the asphaltene molecules can precipitate due to their high density and molecular weight. The precipitation rate begins to decrease after the bubble point pressure due to the release and separation of the gas from the oil. Thus, the oil is dense, and the asphaltene molecules cannot collect and precipitate due to the close density and molecular weight as they return to dissolution in the oil.

For future work, The three models of asphaltene precipitation can be applied to predict asphaltene deposition along the total production system by linking them to the particle transport model, multiphase flow model, and deposition model of asphaltene.

NOMENCLATURE

Symbol	Description	Symbol	Description
a	Equation of state parameter	T_c	Critical temperature, ˚C
b	Equation of state parameter	v	Volume, ft^3
c	Equation of state parameter	X_{Ai}	The mole fraction of site-A in molecule i is not bonded to any other site/s
g	Radial distribution function	x_i	Mole fraction of component i
p	Pressure, psia	z	A mole fraction of the fluid
p_c	Critical pressure, psia	ρ	Density, Ib/ft^3
R	Universal gas constant	ω	Acentric factor
T	Temperature, ˚C		

Acknowledgements

This work was supported by the Department of Oil and Gas Engineering, University of Technology, by covering the cost of publishing, and by the University of Baghdad, College of Engineering, by providing free access to the OnePetro library to obtain the required references.

Credit Authorship Contribution Statement

Ali A. Ali: Writing – review & editing, Writing – original draft, Validation, Software, Methodology.
Ghassan H. Abdul-Majeed: Writing –review & editing, Visualization, Supervision

Declaration of Competing Interest

The authors declare that they have no known competing financial interests or personal relationships that could have appeared to influence the work reported in this paper.

REFERENCES

Abdulwahab, A.H., Aziz, B., and Khidhir, D., 2020. A study of asphaltene precipitation problem in some wells in Kurdistan region. *UKH Journal of Science and Engineering*, *4*(6), pp. 27–36. https://doi.org/10.25079/ukhjse.v4n1y2020.pp27-36.

Afshari, S., Kharrat, R., and Ghazanfari, M.H., 2010, June 8. Asphaltene precipitation study during natural depletion at reservoir conditions. in Proceedings *International Oil and Gas Conference and Exhibition in China, Beijing, China, June 8–10.* https://doi.org/10.2118/130071-MS.

Ahmed, M.A., Abdul-Majeed, G.H., and Alhuraishawy, A.K., 2023a. Asphaltene precipitation investigation using screening techniques for crude oil samples from the Nahr-Umr formation/Halfaya oil field. *Iraqi Journal of Chemical and Petroleum Engineering*, *24*(1), pp. 41–50. https://doi.org/10.31699/IJCPE.2023.1.6.

Ahmed, M.A., Abdul-Majeed, G.H., and Alhuraishawy, A.K., 2023b. Modeling of asphaltene precipitation using CPA-EOS for olive oil in an Iraqi oil well. *AIP Conference Proceedings,* 16–17 July 2022, Pune, India, 2839(1), pp. 28. https://doi.org/10.1063/5.0167684.

Alhuraishawy, A.K., Abdul-Majeed, G.H., and Ahmed, M.A., 2023. Asphaltene stability investigation for crude oil sample from the Nahr-Umr formation/Halfaya oil field. *Iraqi Journal of Oil and Gas Research*, *3*(2). http://doi.org/10.55699/ijogr.2023.0302.1043.

Ali, A.A., 2021. Prediction of asphaltene precipitation behavior of Khasib formation / Halfaya oil field. *Iraqi Journal of Oil and Gas Research (IJOGR)*, *1*(1), pp. 82–95. https://doi.org/10.55699/ijogr.2021.0101.1006.

Ali, A.A., Al-Jawad, M.S., and Ali, A.A., 2019. Asphaltene precipitation modeling of Sadi formation in Halfaya Iraqi oil field. *Journal of Engineering*, *25*(8), pp. 113–128. https://doi.org/10.31026/j.eng.2019.08.08.

Ali, A.A., Al-Jawad, M.S., and Ali, A.A., 2019b. Asphaltene stability of some Iraqi dead crude oils. *Journal of Engineering*, *25*(3), pp. 53–67. https://doi.org/10.31026/j.eng.2019.03.05.

Ali, N.M., and Naife, T.M., 2021. Deasphalting of atmospheric Iraqi residue using different solvents.

Journal of Engineering, *27*(5), pp. 17–27. https://doi.org/10.31026/j.eng.2021.05.02.

Alian, S.S., Alta'ee, A.F., Omar, A.A., and Hani, I., 2011. Study of asphaltene precipitation during CO2 injection for Malaysian light oil reservoirs. In Proceedings *2011 National Postgraduate Conference, 19-20 September 2011, Perak, Malaysia*, pp. 1–5. https://doi.org/10.1109/NatPC.2011.6136535.

Alves, I.N., Caetano, E.F., Minami, K., and Shoham, O., 1991. Modeling annular flow behavior for gas wells. *SPE Production Engineering*, *6*(4), pp. 435–440. https://doi.org/10.2118/20384-PA.

Arya, A., Liang, X., von Solms, N., and Kontogeorgis, G.M., 2016. Modeling of asphaltene onset precipitation conditions with cubic plus association (CPA) and perturbed chain statistical associating fluid theory (PC-SAFT) equations of state. *Energy & Fuels*, *30*(8), pp. 6835–6852. https://doi.org/10.1021/acs.energyfuels.6b00674.

Buenrostro-Gonzalez, E., Lira-Galeana, C., Gil-Villegas, A., and Wu, J., 2004. Asphaltene precipitation in crude oils: Theory and experiments. *AIChE Journal*, *50*(10), pp. 2552–2570. https://doi.org/10.1002/aic.10243.

Comer, T., and Weller, M., 2019. Final PVT analysis report.

Duda, Y., and Lira-Galeana, C., 2006. Thermodynamics of asphaltene structure and aggregation. *Fluid Phase Equilibria*, *241*(1–2), pp. 257–267. https://doi.org/10.1016/j.fluid.2005.12.043.

Farhan, L.W., Almahdawi, F.H.M., and Hammadi, A.S., 2020. Dissolving precipitated asphaltenes inside oil reservoirs using local solvents. *Iraqi Journal of Chemical and Petroleum Engineering*, *21*(1), pp. 45–52. https://doi.org/10.31699/IJCPE.2020.1.7.

Firoozabadi, A., 1999. *Thermodynamics of hydrocarbon reservoirs*. 1st Edition. McGraw Hill.

Gonzalez, D.L., Ting, P.D., Hirasaki, G.J., and Chapman, W.G., 2005. Prediction of asphaltene instability under gas injection with the PC-SAFT equation of state. *Energy & Fuels*, *19*(4), pp. 1230–1234. https://doi.org/10.1021/ef049782y.

Hajizadeh, N., Moradi, G., and Ashoori, S., 2020. Modified SRK equation of state for modeling asphaltene precipitation. *International Journal of Chemical Reactor Engineering*, *18*(3). https://doi.org/10.1515/ijcre-2019-0180.

Hasan, R.M., and A. Al-haleem, A., 2020. Modifying an equation to predict the asphaltene deposition in the Buzurgan oil field. *Iraqi Journal of Chemical and Petroleum Engineering*, *21*(4), pp. 49–55. https://doi.org/10.31699/IJCPE.2020.4.6.

Hasanvand, M., and Kharat, R., 2014. The Thermodynamic modeling of asphaltene precipitation equilibrium during the natural production of crude oil: The role of pressure and temperature. *Petroleum Science and Technology*, *32*(13), pp. 1578–1585. https://doi.org/10.1080/10916466.2011.613431.

Hirschberg, A., DeJong, L.N.J., Schipper, B.A., and Meijer, J.G., 1984. Influence of temperature and pressure on asphaltene flocculation. *Society of Petroleum Engineers Journal*, *24*(03), pp. 283–293. https://doi.org/10.2118/11202-PA.

Izadpanahi, A., Azin, R., Osfouri, S., and Malakooti, R., 2019. Modeling of asphaltene precipitation in a light oil reservoir with high producing GOR: case study. *Advanced NanoMaterials and Technologies for Energy Sector*, 3, pp. 270–279.

Jamaluddin, A.K.M., Creek, J., Kabir, C.S., McFadden, J.D., D'Cruz, D., Manakalathil, J., Joshi, N., and Ross,

B., 2002. Laboratory techniques to measure thermodynamic asphaltene instability. *Journal of Canadian Petroleum Technology*, *41*(07), pp. PETSOC-02-07-04. https://doi.org/10.2118/02-07-04.

Kasim, Z.T., and Abbas, R.K., 2022. Using special additives for decreasing the asphaltene content of Missan crude oil. *Al-Qadisiyah Journal for Engineering Sciences*, *15*(3), pp. 171–178. https://doi.org/10.30772/qjes.v15i3.830.

Kontogeorgis, G.M., V. Yakoumis, I., Meijer, H., Hendriks, E., and Moorwood, T., 1999. Multicomponent phase equilibrium calculations for water–methanol–alkane mixtures. Fluid Phase Equilibria,158–160, pp. 201–209. https://doi.org/10.1016/S0378-3812(99)00060-6.

Kontogeorgis, G.M., Voutsas, E.C., Yakoumis, I. V., and Tassios, D.P., 1996. An equation of state for associating fluids. Industrial & Engineering Chemistry Research, 35(11), pp. 4310–4318. https://doi.org/10.1021/ie9600203.

Li, Z., and Firoozabadi, A., 2010. Modeling asphaltene precipitation by n-alkanes from heavy oils and bitumens using cubic-plus-association equation of state. *Energy & Fuels*, *24*(2), pp. 1106–1113. https://doi.org/10.1021/ef9009857.

Maddah, Z.H., and Naife, T.M., 2019. Demulsification of water in Iraqi crude oil emulsion. *Journal of Engineering*, *25*(11), pp. 37–46. https://doi.org/10.31026/j.eng.2019.11.03.

Mohammed, S.A.M., and Maan, S.D., 2016. The effect of asphaltene on the stability of Iraqi water in crude oil emulsions. *Iraqi Journal of Chemical and Petroleum Engineering*, *17*(2), pp. 37–45. https://doi.org/10.31699/ijcpe.2016.2.5.

Pfeiffer, J.P., and Saal, R.N.J., 1940. Asphaltic bitumen as colloid system. *The Journal of Physical Chemistry*, *44*(2), pp. 139–149. https://doi.org/10.1021/j150398a001.

Robinson, D.B., and Peng, D.-Y., 1978. The characterization of the heptanes and heavier fractions for the GPA Peng-Robinson programs. In TA - TT - Gas Processors Association Tulsa, Okla. https://worldcat.org/title/8631899.

Shirani, B., Nikazar, M., Naseri, A., and Mousavi-Dehghani, S.A., 2012. Modeling of asphaltene precipitation utilizing association equation of state. *Fuel*, *93*, pp. 59–66. https://doi.org/10.1016/j.fuel.2011.07.007.

Shoukry, A.E., El-Banbi, A.H., and Sayyouh, H., 2020. Enhancing asphaltene precipitation modeling by cubic-PR solid model using thermodynamic correlations and averaging techniques. *Petroleum Science*, *17*(1), pp. 232–241. https://doi.org/10.1007/s12182-019-00377-1.

Soave, G., 1972. Equilibrium constants from a modified Redlich-Kwong equation of state. Chemical Engineering Science, 27(6), pp. 1197–1203. https://doi.org/10.1016/0009-2509(72)80096-4.

Tavakoldavani, M., and Ashoori, S., 2017. Determination of asphaltene deposition profile in a wellbores column of one Iranian oil reservoir. *Journal of Applied Environmental and Biological Sciences*, *7*(4), pp. 156–164.

Tharanivasan, A.K., Svrcek, W.Y., Yarranton, H.W., Taylor, S.D., Merino-Garcia, D., and Rahimi, P.M., 2009. Measurement and modeling of asphaltene precipitation from crude oil blends. *Energy and Fuels*, *23*(8), pp. 3971–3980. https://doi.org/10.1021/ef900150p.

Vafaie-Sefti, M., Mousavi-Dehghani, S.A., and Mohammad-Zadeh, M., 2003. A simple model for asphaltene deposition in petroleum mixtures. *Fluid Phase Equilibria*, *206*(1–2), pp. 1–11. https://doi.org/10.1016/S0378-3812(02)00301-1.

Vakili-Nezhaad, G., 2013. Effect of fluid viscosity on asphaltene deposition rate during turbulent flow in oil wells. *American Journal of Chemical Engineering*, *1*(2), pp. 45. https://doi.org/10.11648/j.ajche.20130102.13.

Victorov, A.I., and Firoozabadi, A., 1996. Thermodynamic micellization model of asphaltene precipitation from petroleum fluids. *AIChE Journal*, *42*(6), pp. 1753–1764. https://doi.org/10.1002/aic.690420626.

Wu, J., Prausnitz, J.M., and Firoozabadi, A., 1998. Molecular-thermodynamic framework for asphaltene-oil equilibria. *AIChE Journal*, *44*(5), pp. 1188–1199. https://doi.org/10.1002/aic.690440516.

Wu, J., Prausnitz, J.M., and Firoozabadi, A., 2000. Molecular thermodynamics of asphaltene precipitation in reservoir fluids. *AIChE Journal*, *46*(1), pp. 197–209. https://doi.org/10.1002/aic.690460120.

Zhang, X., Pedrosa, N., and Moorwood, T., 2012. Modeling asphaltene phase behavior: comparison of methods for flow assurance studies. *Energy & Fuels*, *26*(5), pp. 2611–2620. https://doi.org/10.1021/ef201383r.

نمذجة ترسيب الإسفلتين – الجزء الثاني: دراسة مقارنة لطرق التنبؤ بمنحنيات ترسيب الإسفلتين

علي انور علي[1، 2، *]، غسان حميد عبدالمجيد[3]

[1]قسم هندسة النفط، كلية الهندسة، جامعة بغداد، بغداد، العراق
[2]قسم تكنولوجيا النفط، الجامعة التكنولوجية، بغداد، العراق
[3]كلية الهندسة، جامعة بغداد، بغداد، العراق

الخلاصة

كثيرا ما تتأثر قابلية ذوبان الأسفلتين في النفوط الخام بتغيرات درجة الحرارة والضغط وتركيب النفط. وقد يؤدي ذلك إلى ترسيب وتصلب الإسفلتين في أجزاء مختلفة من منظومة الإنتاج الكلي، الأمر الذي من شأنه أن يتسبب في تراجع الإنتاج ويكون له أثر اقتصادي كبير. التنبؤ بظروف ترسيب الإسفلتين سيكون مفيدًا جدًا في حالتين. في الحالة الأولى، وبدون حدوث المشكلة، سيكون من المفيد تحديد ظروف التشغيل المثلى لعمليات إنتاج النفط. وفي الحالة الثانية، مع حدوث المشكلة، سيكون نموذج التنبؤ مفيداً في معرفة مناطق التصلب وأحجامها. هذه الدراسة هي استمرار للجزء الأول، حيث يتم عرض الإصدارات المتقدمة من معادلات Peng-Robinson (APR78 EOS) و Soave-Redlich-Kwong (ASRK EOS) الحالة المكعبة ومعادلات الحالة المكعبة زائد الترابط (CPA EOS). وتمت مقارنتها في التنبؤ بظروف ترسيب الإسفلتين باستخدام برنامج Multiflash. تركزت هذه الدراسة على التنبؤ بمنحنى تركيز الاسفلتين مقابل الضغط لنفط خام حي (API = 24°API) من حقل نفط عراقي عند درجات حرارة مختلفة. البيانات المطلوبة لهذه الدراسة هي التحليل التركيبي، وتجارب PVT، وتحليل SARA، وبيانات ضغط بداية ترسب الإسفلتين، والتي تم جمعها من تقرير تحليل السوائل واستخدامها في البرنامج. ولوحظ أن التطابق كان كبيرا جداً بين ASRK EOS وCPA EOS لجميع قيم درجات الحرارة وابتعدا عن نموذج APR78 EOS في التنبؤ بمنحنى الترسيب عند درجات الحرارة المنخفضة (T = 50 و40 درجة مئوية). المساهمة الرئيسية لهذه الدراسة هي إظهار تأثير اختيار النموذج المناسب في التنبؤ بالترسيب الإسفلتيني وكيف ستؤثر هذه المرحلة على التنبؤات المستقبلية أو الإضافية لمشكلة التصلب الإسفلتيني.

الكلمات المفتاحية: تركيز ترسب الإسفلتين، ضمان التدفق، ضغط بداية ترسب الإسفلتين، معادلة الحالة المكعبة.